The Los Alamos Sferic Array: A research tool for lightning investigations

D. A. Smith, K. B. Eack,[1] J. Harlin,[1] M. J. Heavner, A. R. Jacobson,
R. S. Massey,[2] X. M. Shao, and K. C. Wiens[3]

Space and Atmospheric Sciences, Los Alamos National Laboratory, Los Alamos, New Mexico, USA

[1] Since 1998 the Los Alamos Sferic Array (LASA) has recorded electric field change signals from lightning in support of radio frequency (RF) and optical observations by the Fast On-orbit Recording of Transient Events (FORTE) satellite. By ''sferic'' (a colloquial abbreviation for ''atmospheric''), we refer to a remote measurement of the transient electric field produced by a lightning flash. LASA consisted of five stations in New Mexico in 1998 and was expanded to 11 stations in New Mexico, Texas, Florida, and Nebraska in 1999. During the 2 years of operation described in this paper, the remote stations acquired triggered 8- or 16-ms duration, 12-bit waveforms and GPS-based sferic time tags 24 hours per day year-round. Source locations were determined daily using differential time of arrival techniques, and the waveforms from all geolocated events were transferred to Los Alamos National Laboratory (LANL), where they have been archived for further analysis, including event classification and characterization. We evaluated LASA location accuracy by comparing temporally coincident (occurring within 100 μs) LASA and National Lightning Detection Network (NLDN) event locations. Approximately one half of the locations agreed to within 2 km, with better agreement for events that occurred within the confines of LASA subarrays in New Mexico and Florida. Of the ∼900,000 events located by the sferic array in 1998 and 1999, nearly 13,000 produced distinctive narrow bipolar field change pulses resembling those previously identified as intracloud discharges. *INDEX TERMS:* 3324 Meteorology and Atmospheric Dynamics: Lightning; 3304 Meteorology and Atmospheric Dynamics: Atmospheric electricity; 6934 Radio Science: Ionospheric propagation (2487); 6904 Radio Science: Atmospheric propagation; *KEYWORDS:* lightning, RF, sferic array, FORTE

1. Introduction

[2] The Los Alamos Sferic Array (LASA) was developed to perform lightning research in support of the Fast On-orbit Recording of Transient Events (FORTE) satellite. The purpose of FORTE, which was launched into a 69° inclination, 800-km orbit in August of 1997, has been to study transient VHF radio and optical emissions from the Earth for the purpose of nuclear weapon monitoring research. FORTE's primary research payloads include two 22-MHz bandwidth RF receivers, one 85-MHz bandwidth RF receiver, a broadband optical CCD imager, and a narrowly filtered optical photodiode detector. These instruments regularly record the radio and optical emissions from terrestrial lightning discharges. FORTE RF payloads and observations have previously been described by *Massey et al.* [1998a],

Jacobson et al. [1999, 2000], and *Suszcynsky et al.* [2000]. Optical payloads, observations, and modeling have been described by *Kirkland et al.* [1998], *Suszcynsky et al.* [1999], *Light et al.* [2001], and *Suszcynsky et al.* [2000, 2001].

[3] A significant fraction of the FORTE science effort has focused on merging FORTE RF and optical observations with those from other satellite- and ground-based resources. This data fusion has enhanced the value of FORTE observations in at least three respects: (1) Sensors with the ability to accurately geolocate sources have provided locations for events that FORTE has recorded but been unable to locate (FORTE's limited geolocation capabilities have been described by *Jacobson et al.* [1999], *Suszcynsky et al.* [2001], *Jacobson and Shao* [2000], and *Shao and Jacobson* [2001]); (2) multiple characterizations of the same stroke, flash, or storm using different sensor types have provided insight into thunderstorm electrification and discharge processes that no single sensor has been able to provide; and (3) sensors capable of continuously observing storms have provided a context for FORTE data collection, which is limited to the observation of a single location on the ground for only 15 min (at most) per 100-min orbit, with no guarantee of observing the same location on the subsequent orbit.

---

[1] Now at Department of Physics, New Mexico Institute of Mining and Technology, Socorro, New Mexico, USA.
[2] Deceased March 5, 1999.
[3] Now at Department of Atmospheric Science, Colorado State University, Fort Collins, Colorado, USA.

Table 1. Los Alamos Sferic Array Stations, Locations, and Dates of Operation

Station ID	Initial Date of Operation	Location	Host Facility
LA	Apr. 6, 1998	Los Alamos, NM	Los Alamos National Laboratory
SO	May 1, 1998	Socorro, NM	New Mexico Tech
RO	May 12, 1998	Roswell, NM	Eastern New Mexico University
TU	May 27, 1998	Tucumcari, NM	Mesa Technical College
LO[a]	July 1, 1998	Los Alamos, NM	Los Alamos National Laboratory
CR	Feb. 9, 1999	Omaha, NE	Creighton University
KC	April 5, 1999	Cape Canaveral, FL	Kennedy Space Center
TA	April 6, 1999	Tampa, FL	University of South Florida
FM	April 8, 1999	Fort Myers, FL	Cyberstreet ISP
BR	April 8, 1999	Boca Raton, FL	Florida Atlantic University
GV	April 9, 1999	Gainesville, FL	University of Florida
LB	April 27, 1999	Lubbock, TX	Texas Tech University

[a] LO station was second of two in Los Alamos during 1998. It was decommissioned on August 11, 1998.

[4] An example of a resource that has been used to supplement FORTE data analysis is the National Lightning Detection Network (NLDN) [*Cummins et al.*, 1998a], which has played a role in the processing of FORTE data acquired over the conterminous United States (CONUS). The NLDN provided locations, event identifications, and peak current estimates for nearly 15,000 FORTE-coincident events in 1998 [*Jacobson et al.*, 2000] and over 10,000 in 1999 (A. R. Jacobson, private communication, 2000). Other resources that have been utilized for FORTE comparative analyses include the Kennedy Space Center (KSC) Lightning Detection and Ranging (LDAR) system [*Lennon and Maier*, 1991], New Mexico Tech Lightning Mapping Array (LMA) [*Rison et al.*, 1999b], optical imagers on board the NASA MicroLab-1 and Tropical Rain Forest Measuring Mission (TRMM) satellites, the Brazilian Lightning Detection Network (BLDN) [*Pinto et al.*, 1999], space-based visible and IR imagers (e.g., GOES), and the Next Generation Weather Radar (NEXRAD) surveillance network.

[5] The Los Alamos Sferic Array was developed as a resource for locating, classifying, and characterizing lightning discharges in support of FORTE. One advantage of operating our own ground-based array has been our ability to tailor operations for coordination with FORTE in order to maximize the likelihood of making coincident observations. A second advantage has been our ability to retain all waveforms from all located events to permit detailed reanalysis of data. This brute-force approach to data archiving has allowed us to evolve and optimize our processing techniques and to apply them back to a large collection of ground-based sferic and satellite-based RF waveforms. As we have advanced our understanding of the lightning data and developed new questions, the ability to reprocess these waveform data has been of greater value than if we had retained only waveform parameters.

[6] Conceptually, LASA is an expansion of the three-station array utilized by *Smith et al.* [1999a] [see also *Smith*, 1998] to make observations of compact intracloud discharges (CIDs) and other lightning electrical discharges in New Mexico and west Texas during the summer of 1996. The success of both the previous array and the current array have been made possible by the marriage of a well-established sensor technology, the electric field change meter [*Krehbiel et al.*, 1979], with the modern-day capability to derive accurate, absolute time tags at multiple, distant locations using GPS (Global Positioning System) receivers. The Los Alamos National Laboratory (LANL) sferic array has additionally made extensive use of the Internet to cost-effectively manage multiple, unattended sensors and to retrieve hundreds to thousands of megabytes of waveform data on a daily basis.

[7] The purpose of this paper is three-fold: (1) to describe the implementation and operation of the Los Alamos Sferic Array during its first two years in service; (2) to present an evaluation of its geolocation accuracy through comparison with the NLDN; and (3) to introduce initial results on the topic of automatic classification of narrow bipolar pulses (NBPs) in the LASA database. By NBPs we refer to the distinct class of electric field change waveforms described by *Le Vine* [1980], *Willett et al.* [1989], and *Smith et al.* [1999a] that are accompanied by very powerful HF and VHF radiation and that have been associated with CIDs [*Smith*, 1998].

2. Instrumentation

2.1. Array Overview

[8] We began operation of the Los Alamos Sferic Array with five stations (only four of which were independently located) in New Mexico in 1998. The stations were located in Los Alamos (two stations), Socorro, Roswell, and Tucumcari. In 1999 the array was expanded to 11 stations (all independently located), with four stations in New Mexico (in the previously mentioned locations); one in Omaha, Nebraska; one in Lubbock, Texas; and five in Florida in the following locations: Kennedy Space Center, Tampa, Fort Myers, Boca Raton, and Gainesville. Table 1 lists the field change station locations, the two-letter station identifiers used throughout this paper, the host facilities, and the starting dates of operation. Figure 1 is a map of the 1998 and 1999 LASA station locations.

[9] As shown in Figure 1, the 1998 array stations (represented as squares) approximately formed a square with ~200 km separating the stations along the perimeter. The configuration was excellent for lightning studies in and near the state of New Mexico.

[10] The 1999 array consisted of two five-sensor station clusters, one in New Mexico/Texas (referred to as the NM subarray) and one in Florida (the FL subarray), with one additional, outlying station in Nebraska (NE) for a total of
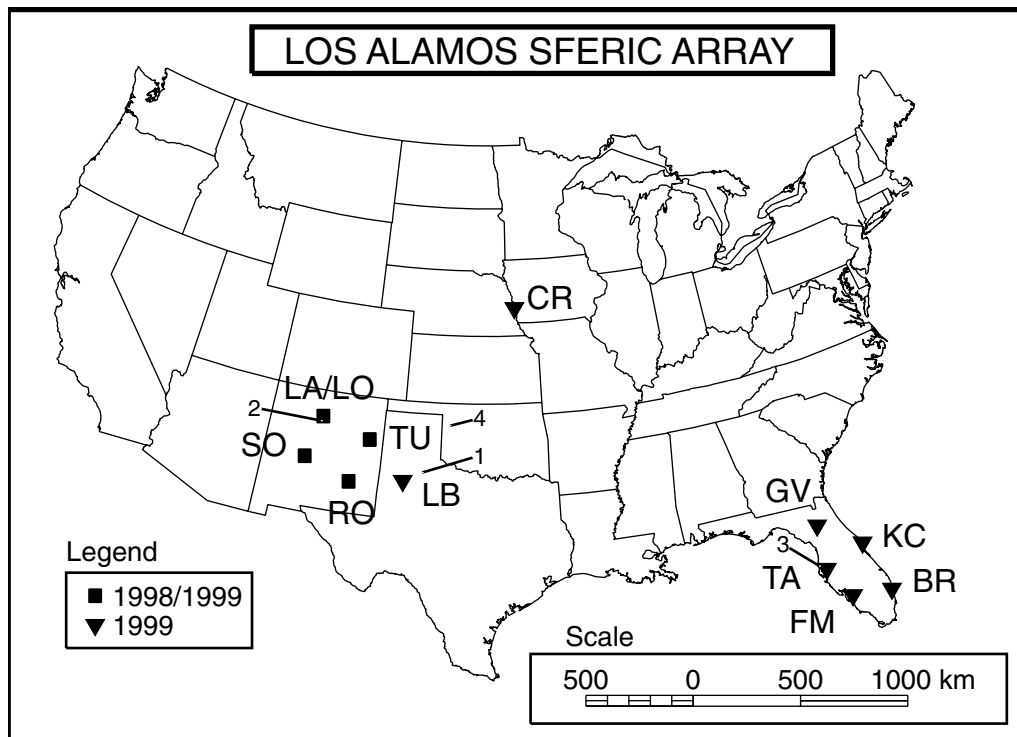
Figure 1. Map showing locations of the 1998 and 1999 Los Alamos Sferic Array stations. Numerals "1" through "4" indicate the locations of lightning discharges described in this paper.

11 stations. The baselines for the NM and FL subarrays were between 160 and 240 km. Utilizing the two subarrays plus the additional station in NE, we were able to perform high-sensitivity, high-location-accuracy studies within and near each subarray and were simultaneously able to detect and locate (with less accuracy) large-amplitude events that occurred over a large portion of the southern and central United States.

[11] Except where footnoted in Table 1 and during temporary computer or network outages, LASA stations were operated 24 hours per day from their starting dates through the end of 1999 (and beyond, but this paper addresses only the 1998/1999 data).

[12] The primary goals for 1998 were to support FORTE and to gain experience in the remote operation of an array by establishing field change stations close to Los Alamos. The nearby locations simplified the deployment and servicing of the stations and also allowed us to make comparative observations with the New Mexico Tech LMA, which was operated in the vicinity of Socorro during the latter part of the 1998 thunderstorm season (and also in 1999). *Rison et al.* [1999a, 1999b] have described joint LASA/LMA observations of NBPs that were made during this campaign.

[13] The expansion to Florida in 1999 was motivated by the following factors: (1) The Florida peninsula features the highest flash density in the United States [*Cummins et al.*, 1998b]; (2) the location provided us with the opportunity to make thunderstorm observations in a maritime environment; (3) for operational reasons related to the locations of the FORTE ground stations (in Albuquerque, New Mexico, and Fairbanks, Alaska), the FORTE satellite was capable of spending more time acquiring data over Florida than over

New Mexico, increasing the likelihood of achieving LASA/ FORTE coincidental detections; and (4) the LDAR system at KSC, which produces accurate, highly resolved, three-dimensional (3-D) maps of lightning RF sources within ~100 km of Cape Canaveral [*Boccippio et al.*, 2001], is located on the perimeter of the Florida sferic subarray and is available for joint lightning studies.

[14] The Nebraska station was installed and made operational in 1998, but was not incorporated into daily LASA processing until 1999. It was originally deployed to support sprite research in the Great Plains region of the United States, but has since proven to be useful for long-range studies of lightning discharges in general.

2.2. Station Description

[15] The requirements for LASA site locations include a relatively quiet noise environment at VLF/LF radio frequencies, access to AC power and a high-speed Internet connection in close proximity to an outdoor rooftop location, and the existence of a cooperative host institution and/ or individual. Of these, the requirement for an Internet connection generally presented the most serious restriction on potential sites.

[16] Figure 2 is a block diagram of a LASA electric field change installation. All stations were identical in configuration except for the low-pass and high-pass signal filters, which were added in 1999 and were not the same for all stations. Figure 3 is a photograph of the array station at the University of Florida in Gainesville. The "inverted salad bowl" or "hairdryer" design was adapted from a design by M. Brook of New Mexico Tech and was previously described by *Smith et al.* [1999a]. The stainless steel dome
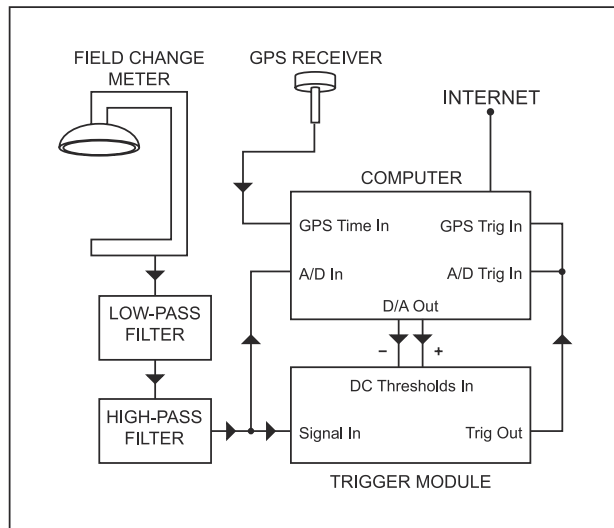
Figure 2. Block diagram of a Los Alamos Sferic Array station.

suspended from the "neck" of the field change meter in Figure 3 shields a 38-cm-diameter sensing plate from precipitation. Without the dome the sensor would be susceptible to spurious signals produced by the impact of charged raindrops on the sensing plate. A charge amplification circuit inside the dome was fed from the sensing plate and configured with a 1-ms decay time constant. A 50-Ω line driver sent the field change output signal through 30 m (typically) of coaxial cable to the interior of the building. Rising from the neck of the field change meter in Figure 3 is the GPS antenna/receiver for the station. It interfaces with the computer inside the building to provide absolute (UTC) event time tagging with a maximum error of 2 μs.

[17] As mentioned earlier, the low-pass and high-pass signal filters were added in 1999. The low-pass filters had a cutoff frequency of 500 kHz and were inserted to prevent aliasing by the 1-megasample/s waveform digitizer. We had previously concluded that the antialiasing filters were not necessary due to a roll-off in the field change meter frequency response above the Nyquist sampling frequency. However, at two of the stations the roll-offs were not steep enough to prevent transmissions from powerful local AM radio stations (with center frequencies near 1 MHz) from aliasing into the digitized sferic waveforms. The low-pass filters greatly reduced the interference problem. The single-pole high-pass filters were added in 1999 to eliminate DC offsets in the outputs at some of the Florida stations (possibly caused by leakage current due to high humidity) and also to mitigate a 60-Hz noise problem at the Fort Myers station. The 3-dB cutoff frequencies at all stations except Fort Myers (FM) were 34 Hz. The FM cutoff was 340 Hz. The difference has been noticeable in waveforms or waveform segments dominated by lower-frequency signal components, which are more severely attenuated in the FM data. Note that the external high-pass filters act in addition to the ~1-kHz high-pass effect resulting from the 1-ms decay time constant of the field change meter electronics.

[18] The filtered field change signal (refer again to Figure 2) was split between a 12-bit analog-to-digital converter (A/D)

card in the computer and an external trigger module, which was used to implement trigger criteria. The trigger module accepted positive and negative DC thresholds from a digital-to-analog converter (D/A) card in the computer. The two thresholds were separately and remotely adjustable and were used to define the thresholds at which the bipolar trigger circuit would trigger data acquisition. During 1998 the thresholds were adjusted infrequently and simply set to levels that produced comfortable trigger rates. During 1999, a "campaign mode" of operation was implemented to maximize the likelihood of making coincident observations of FORTE-detected events and also to study long-distance sferic propagation. In campaign mode, monthly schedules of threshold changes were sent to the remote stations where resident scheduling programs raised and lowered station thresholds in conjunction with FORTE passes and at other regular time intervals when increased sensitivities were desired. Typical thresholds during campaign mode and noncampaign mode were ±1.5 V/m and ±6 V/m, respectively. Campaign mode increased the likelihood of a given array event being detected by FORTE by a factor of 4 from 0.074% in 1998 to 0.30% in 1999. The total number of FORTE/LASA coincidences for 1998 and 1999 was 2422, where we have defined a coincidence as an event time agreement within ±300 μs after correction for the propagation delay to FORTE.
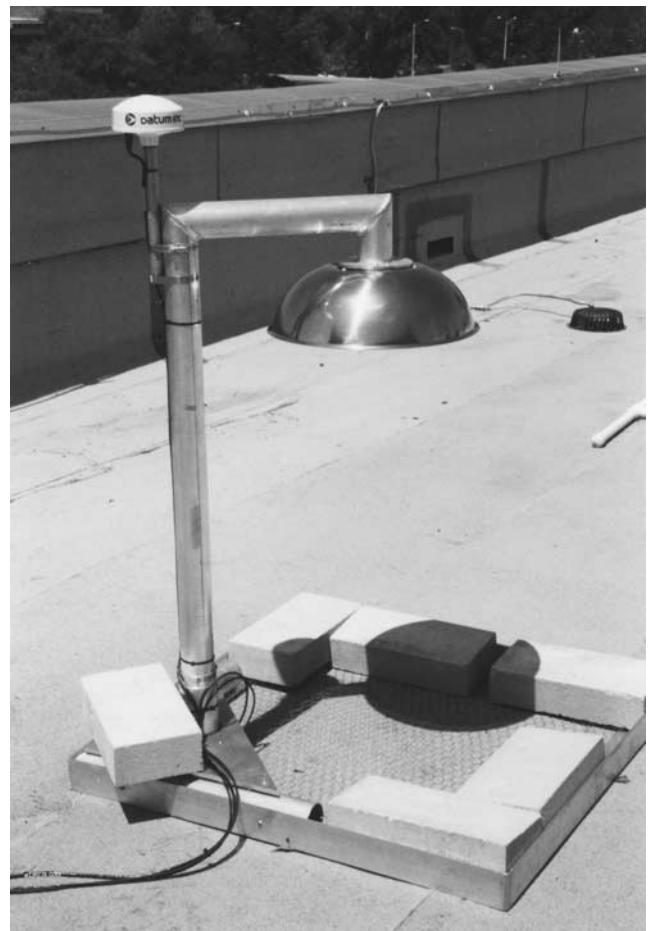

Figure 3. Photograph of the sferic array station at the University of Florida in Gainesville.
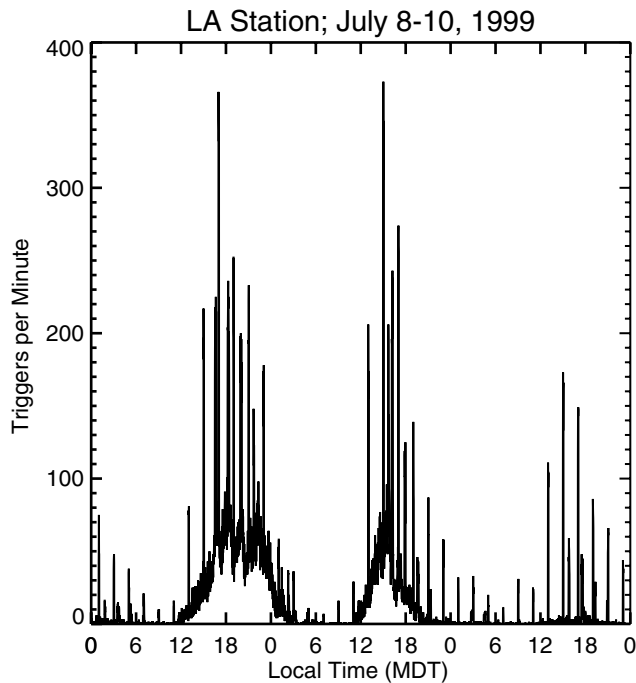
LA Station; July 8-10, 1999

Figure 4. Plot of the trigger rate as a function of time (mountain daylight time) for the Los Alamos array station during 3 days of activity during the summer of 1999. Spikes in the trigger rate are indicative of lowered station thresholds in association with campaign mode.

[19] Figure 4 provides an example of the increased sensitivity at the LA array station during campaign-mode time segments on July 8–10, 1999. The graph shows trigger rate (triggers per minute) as a function of local time of day (mountain daylight time (MDT)) for the 3-day period. Brief (5- to 15-min duration) spikes in the rate correspond to periods of lowered thresholds. Because the station was more sensitive during periods of lowered thresholds, it recorded events associated with weaker and/or more distant lightning activity. Both threshold settings in Figure 4 show a diurnal increase in lightning rate that begins around noon and extends through the early to late evening. The peak rate during high-threshold periods exceeds one event per second. The peak rate during low-threshold periods exceeds six events per second.

[20] Trigger signals from the trigger module were sent to the A/D and GPS cards in the computer, which recorded a field change waveform and time of trigger for each detected event. With the exception of the LO station, all stations acquired 8-ms waveforms sampled at 1 megasample/s during 1998 and 1999. The pretrigger fractions for non-LO stations in 1998 and 1999 were 50% and 25%, respectively. The LO station was operated in 1998 only and acquired 1 megasample/s, 16-ms duration records with 25% pretrigger. The motivation behind the LO station configuration was to search for sprite signatures in waveforms immediately following positive cloud-to-ground (CG) lightning stroke signatures. The dead time between triggers for the individual stations during 1998 ranged from 30 to over 100 ms, depending on the time required to write each waveform to disk. This time was found to be a function of the fullness of the data directory at

each station. In 1999, file handling improvements reduced the dead time between triggers, so that the retrigger time was consistently <40 ms. Reducing the dead time increased the likelihood of detecting subsequent CG return strokes.

[21] Each time a trigger was received by a remote station the corresponding sferic waveform was written to a data file and the UTC time tag (from the GPS receiver) was written to a separate header file, which was used to log daily station time tags. Data acquisition proceeded in this fashion until the UTC day rollover, when data acquisition was automatically stopped and restarted to allow transfer and processing of the previous day's data.

[22] A trigger rate limiter was implemented in software at each remote station to prevent the hard drive from filling up in the event of an extremely high trigger rate resulting from a close lightning storm or the appearance of a new or intermittent noise source. During times when the rate limiter was activated (typically corresponding to a trigger rate of >10 events per second for at least 10 s), waveform acquisition halted but time tag acquisition continued.

[23] During 1998 and 1999 the field change hardware, computers, operating systems, and software functioned reliably. In part because of this reliability and in part because of the cooperation of our colleagues at the remote sites, it was not necessary for LANL personnel to visit the stations at any time for troubleshooting following the establishment of initial station operating capability.

2.3. Array Processing

[24] Like the remote stations, the LANL array-processing computer (APC) operated automatically (without operator intervention) on a daily cycle. The first task following the UT day rollover was to transfer (via the Internet) the previous day's header files from the remote stations to LANL, where temporal coincidences involving a minimum of three stations were identified (three stations are required to make a 2-D source location determination). The width of the coincidence time window was determined by the time required for a radio signal to transit (at the speed of light) the longest chord of the array, since this time represents the largest possible differential time of arrival (DTOA) for a real event. A slightly longer window was implemented in practice to allow for the possibility that stations trigger on the same event, but not on the same waveform feature. In 1998 the window was 2 ms, corresponding to the delay between the RO and LA stations. In 1999 the window for the complete 11-station array was 10 ms, corresponding to the delay between the BR and LA stations.

[25] Having identified the temporal coincidences between array stations, the APC directed the remote computers to compress the coincident waveforms for subsequent retrieval and decompression. Following the retrieval of all data from all stations for the day, waveforms were cross-correlated to determine timing corrections between the events recorded by different stations. In addition to making fine timing corrections, this step was used to reject (on the basis of poor cross-correlation coefficients) waveforms suspected to originate from different sources, i.e., noise recorded by a single sensor or independent, nearly simultaneous (occurring within milliseconds of each other) lightning flashes.
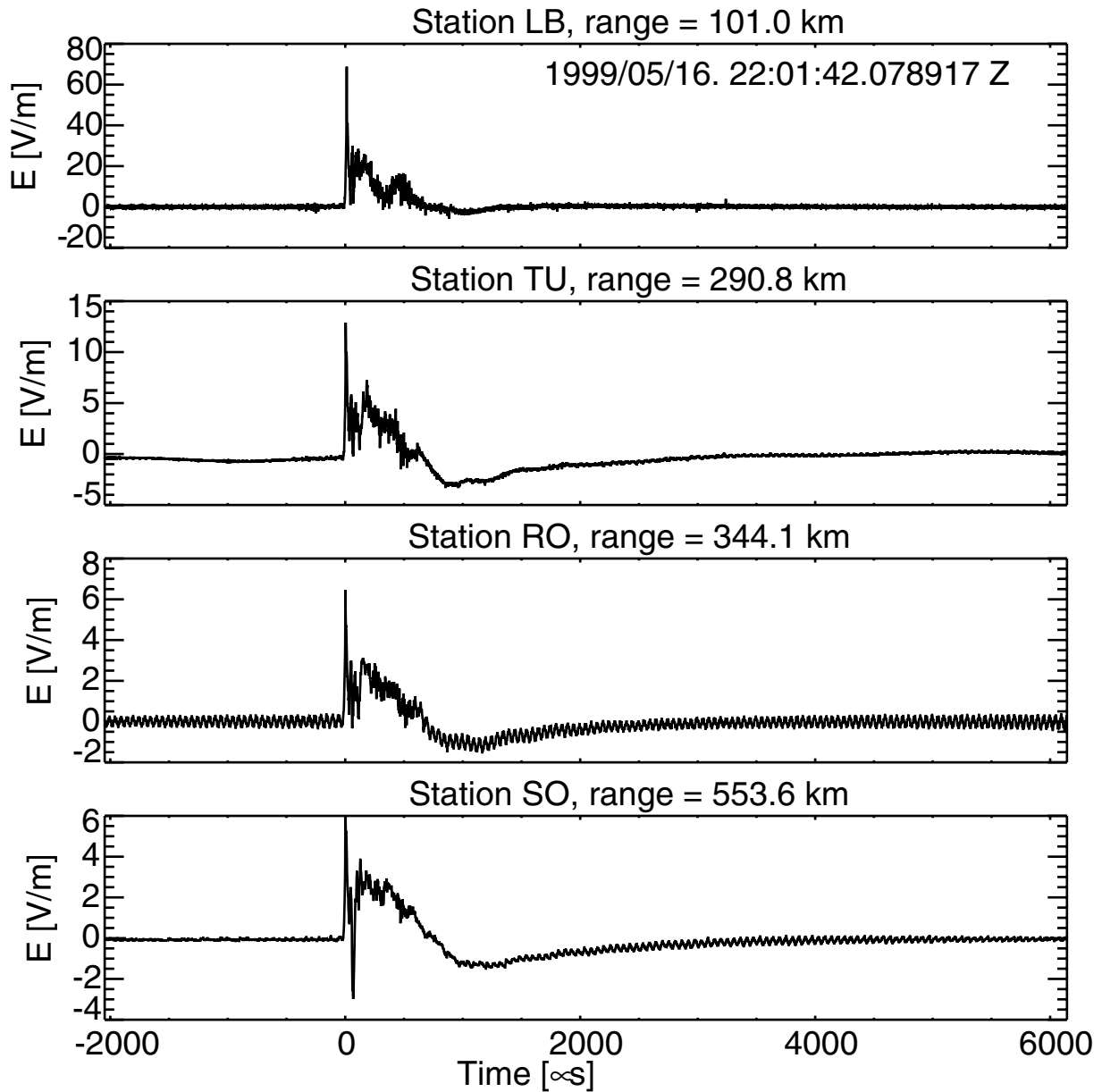
Figure 5. Electric field change waveforms from a positive cloud-to-ground (CG) lightning return stroke that occurred in the Texas Panhandle (the location is indicated by a numeral "1" in Figure 1). The National Lightning Detection Network (NLDN) characterized the stroke as a positive CG with a peak current of 94 kA.

[26] Figure 5 shows multiple waveforms recorded from a single positive CG flash that occurred in the Texas Panhandle on May 16, 1999 (the location is indicated by a "1" in Figure 1). The waveforms were recorded by the LB, TU, RO, and SO stations from ranges of 101, 291, 344, and 554 km, respectively. The waveforms are presented in order from nearest to farthest distance between the sensor and event, as are all waveforms in this paper. The flash was characterized by NLDN as a positive CG with a peak current of 94 kA. The physics polarity convention (indicating current flow from overhead to below) is used throughout this paper. Note that the SO (Figure 5, bottom) waveform features an early/fast negative excursion at the expected single-hop ionospheric delay time (68 μs) given the source range (554 km) and an assumed ionospheric virtual reflection height of 70 km (typical for the late afternoon).

[27] Cross correlations were not performed on the entire 8- or 16-ms sferic waveforms. This was found to be burdensome with regard to computational intensity and also resulted in an occasional missed correlation due to ionospheric reflections or noise. Because most sferic waveforms have a single, prominent feature that lasts less than 1 ms, correlations were performed on 512-point (512 μs) windows centered on the peak absolute waveform amplitudes.

[28] The computed cross-correlation coefficients for the waveforms in Figure 5 were 0.95 (1 and 2), 1.00 (2 and 2),
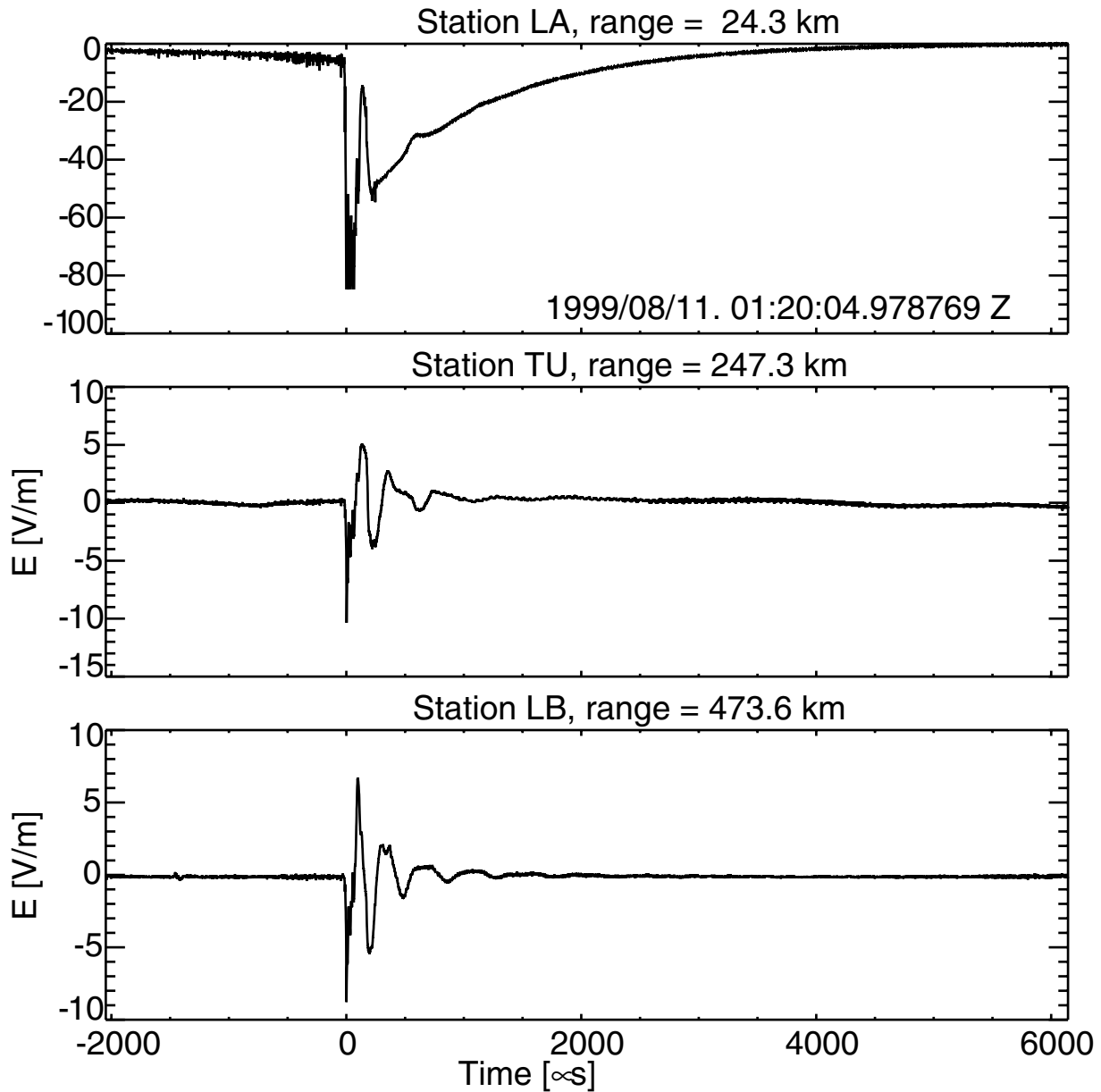
Figure 6. Electric field change waveforms from a negative CG lightning return stroke that occurred 24 km southwest of Los Alamos (the location is indicated by a numeral "2" in Figure 1). The first waveform features an obvious static field component. The NLDN characterized the stroke as a negative CG with a peak current of 54 kA.

0.97 (3 and 2), and 0.85 (4 and 2). As indicated by the unity coefficient for the second waveform, the cross correlations were all performed with respect to the second waveform in time order of arrival. This has been the standard convention for LASA waveform correlation because it guarantees that the template waveform is dominated by the radiation component of the electric field and not by the intermediate or static components, which can seriously affect the field change waveshape within several tens of kilometers of a recording station.

[29] Figure 6 shows waveforms recorded from a negative CG (54 kA peak current as reported by the NLDN) that occurred 25 km southwest of Los Alamos on August 11, 1999, and was recorded by the LA, TU, and LB stations (the event location is indicated by a "2" in Figure 1). The Los Alamos (Figure 6, top) waveform features a large negative shift near time zero that decays to zero over a period of several milliseconds. The shift is from the static component of the electric field, which is superimposed on the radiation and induction field components. The exponential decay following the stroke is a characteristic of the field change meter electronics that allows subsequent strokes or flashes to utilize the same instrumental dynamic range by returning the trace to zero within a few milliseconds. By always performing the cross correlations with respect to the second waveform (except for 1998 events when the first two stations were the colocated LA and LO sensors, in which case we used the third waveform as the template), the
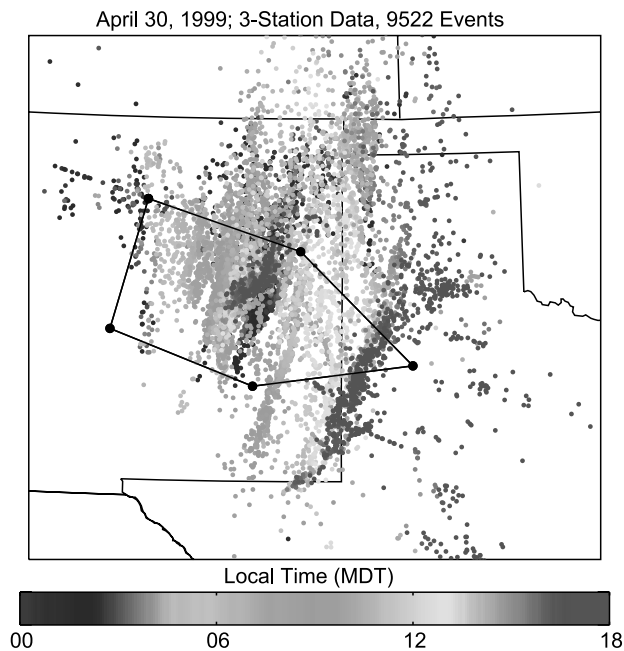
April 30, 1999; 3-Station Data, 9522 Events

Local Time (MDT)

00   06   12   18

Figure 7. Map of array activity recorded in the vicinity of the NM subarray on April 30, 1999. Color is indicative of local time of day (MDT). See color verison of this figure at back of this issue.

template waveform is always recorded from a distance of at least half the length of the shortest array baseline, or ~80 km. Although this convention assures the choice of a reasonable template, it does not address the poor correlations that can result when the first waveform is close to the source. The correlation coefficients for the waveforms in Figure 6 were 0.58, 1.00, and 0.80. The poor (but not unusable) correlation between the first two waveforms results largely from the static component of the LA waveform. As waveforms differ from each other to a greater extent, the time lag adjustments are affected more adversely, which ultimately affects the accuracy of the location solution. The LASA event location for the Figure 6 negative CG differed from the NLDN location by 2.7 km, whereas the typical difference for events within a subarray was <2.0 km (as will be shown later). The NLDN has addressed problems associated with static radiation through a variety of heuristic methods. The NLDN methodology is an appropriate solution for a well-populated and large array, but would lead to the elimination of too many waveforms for LASA. The inclusion of electrostatically influenced waveforms may adversely affect the overall location accuracy of LASA, as discussed in section 3.

[30] As stated earlier, correlation coefficients have been used to eliminate poor waveform matches. The minimum coefficient we accept for first waveform (in time order of arrival, cross-correlated with respect to the second waveform) is 0.20. The minimum we accept for third, fourth, etc., waveforms is 0.55. Waveforms with a significant static component are often rejected for their poor correlation coefficients. When a waveform is rejected and the total number of contributing stations is greater than three, the dissimilar waveform is discarded and the location solution is derived from the remaining stations. When the number of

contributing stations is equal to three, only two waveforms remain after the rejection of the dissimilar waveform, so the event is rejected because three stations are required to locate an event. A final interesting note on Figure 6 is that both static and radiation (and/or intermediate) field terms are observable in the approaching leader prior to the attachment near time zero.

[31] Following waveform cross correlation the events are located by the APC using the correlation-adjusted DTOAs. The location solution is determined using a multidimensional downhill simplex method [*Nelder and Mead*, 1965] called Amoeba [*Press et al.*, 1986]. A similar sferic location method has been described and employed by *Lee* [1989]. Prior to applying the location algorithm the software verifies that the interstation DTOAs are physically possible, i.e., less than the interstation speed-of-light propagation times. Stations with times that do not meet this criterion are rejected from the solution determination. Additionally, three-station events that include both LA and LO (the colocated sensors) are rejected from the database because there exists only one independent DTOA for these cases.

[32] Figure 7 shows a map of event locations in the vicinity of the NM array on April 30, 1999. All events recorded by at least three stations are pictured, with the total event count being nearly 10,000. Colored dots are used to indicate event location as a function of local time of day (MDT) from 0000 to 1800. The NM array station locations are represented by black dots connected by black lines. From the map it is discernable that the lightning was associated with frontal activity since (1) the event rate is more or less constant throughout the day, (2) the activity shows general motion from the northwest, and (3) the events are aligned in a direction generally perpendicular to the apparent storm motion. Air mass thunderstorms, which typically become active later in the spring or summer in New Mexico, generally do not continue to produce intense activity through the late night and into the following morning (as this storm did). The map shows an example of activity occurring in the vicinity of a subarray. Campaign mode was active throughout the day, so station thresholds were varied between ~2 and ~6 V/m. Some of the color banding that is evident is likely due to the threshold variations during FORTE overpasses.

[33] Figure 8 shows a map of event locations on December 12 and 13, 1999, on an expanded spatial scale. At least three wintertime storm systems are visible over the 2-day period during which the thresholds at all stations were left unusually low (0.5 to 1.5 V/m for most stations) for the entire time (no campaign mode). A large frontal thunderstorm system moved from Texas, Oklahoma, and Arkansas through Louisiana and Mississippi and into the Gulf of Mexico. A second large system at a range of over 1500 km from any array stations was active in the North Atlantic Ocean and showed movement toward the east-southeast. Another thunderstorm was active in the Caribbean Sea north of Panama. The location accuracies for such distant storms are discussed in section 3. Events that occurred in the system over the mainland United States were certainly located with better accuracy than events occurring outside of the array, since they were observed with more favorable viewing geometry. Evidence of this is shown by the uniform color variations in the Texas/Louisiana storm compared to
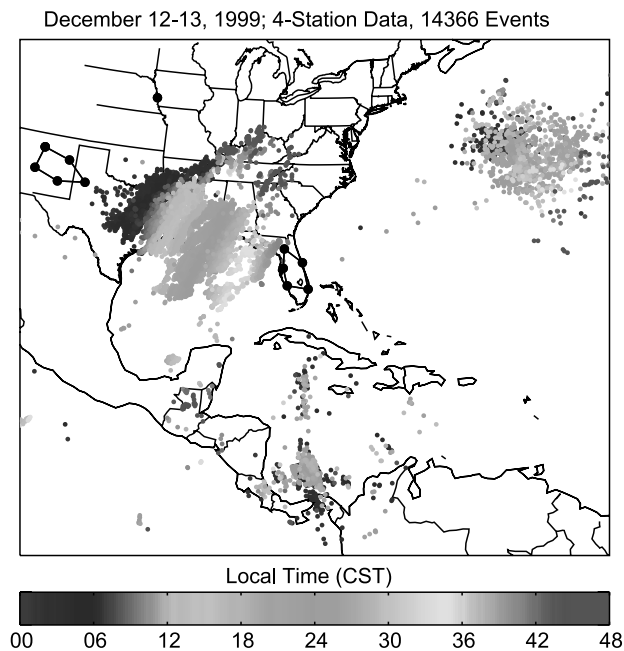
December 12-13, 1999; 4-Station Data, 14366 Events

Local Time (CST)

| 00 | 06 | 12 | 18 | 24 | 30 | 36 | 42 | 48 |

Figure 8. Map of all array activity recorded on December 12–13, 1999. Color is indicative of local time of day (central standard time). The map demonstrates the long-range detection capability of the sferic array when the thresholds are low. See color version of this figure at back of this issue.

the offshore storms. Daily maps similar to those pictured in Figures 7 and 8 were generated automatically and made available via the Internet to assist in array state-of-health monitoring.

3. Array Geolocation Accuracy

3.1. Geolocation Data Analysis

[34] Time-of-arrival lightning location systems, using both low-frequency and high-frequency radio receivers, have been described and utilized by many researchers, including *Proctor* [1971], *Lennon and Maier* [1991], *Cummins et al.* [1998a], *Smith et al.* [1999a], and *Rison et al.* [1999b]. Limits on the location accuracy and precision of such systems depend on the quality of the timing source or sources used to time tag events at each station, the ability to correlate waveforms received by multiple stations, and the source viewing geometry.

[35] To evaluate the location accuracy of the sferic array, we compared LASA event locations to lightning locations determined by the NLDN during 6 months (April–September) in 1998 and 6 months (May–October) in 1999. The NLDN has been described in detail by *Cummins et al.* [1998a, 1998b]. NLDN data products include real time and archival (since 1989) times, locations, and current estimates for lightning return strokes. The network is an operational system that provides uniform coverage of CONUS with a high level of quality control. In contrast, LASA was conceived of as a research system to provide regional acquisition of waveforms for lightning (CG and intracloud) detection, location, and characterization, primarily in support of FORTE. LASA data are neither temporally nor

spatially uniform, so statistical studies are difficult to perform. The array is more useful for single event or storm studies.

[36] The NLDN data sets used for the comparisons in this paper were not standard NLDN data products, but were reprocessed from raw data using relaxed event criteria in order to maximize the detection of both intracloud discharges and distant/weak CG discharges [*Jacobson et al*, 2000]. The standard NLDN data provide 80–90% detection efficiency of first CG strokes with currents of >5 kA within CONUS. These events are located with a median accuracy of 500 m [*Cummins et al.*, 1998a]. The "loosened criteria" data used for comparison in this paper may not meet these quality-control criteria; their uncertainty has not been characterized.

[37] We began the comparison by identifying temporally coincident events in the LASA and NLDN data sets, the purpose being to select probably coincidences based on closeness in time and then to utilize those events for the location comparison. Figure 9 shows a histogram of all 1998/1999 LASA/NLDN time differences over a span of ± 500 μs with a bin size of 5 μs. A significant peak is evident near zero lag, and the noise floor (indicative of random coincidences) is very low (indistinguishable from zero in Figure 9). The total number of events within ± 500 μs is 566,946. The peak occurs at +2 μs, has a half-width of 7 μs (these numbers were determined separately with finer binning), and is slightly asymmetric with a bulge on the right side. The offset and asymmetry (indicative of LASA events that occurred a few to hundreds of microseconds after their corresponding NLDN events) are attributable to multiple factors. The first factor is that the NLDN utilizes a waveform extrapolation to zero amplitude to attempt to time tag the attachment process (or, presumably, the first detected current rise for an
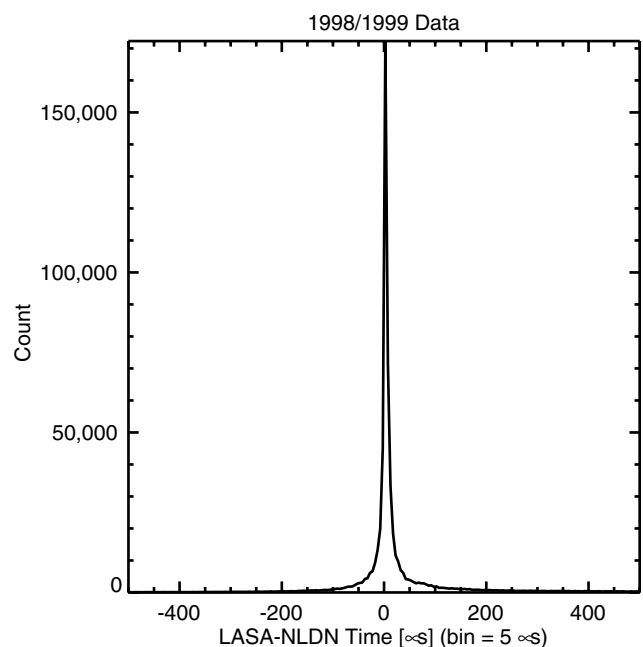
1998/1999 Data

Figure 9. Histogram of LASA/NLDN time differences (1998/1999 data).
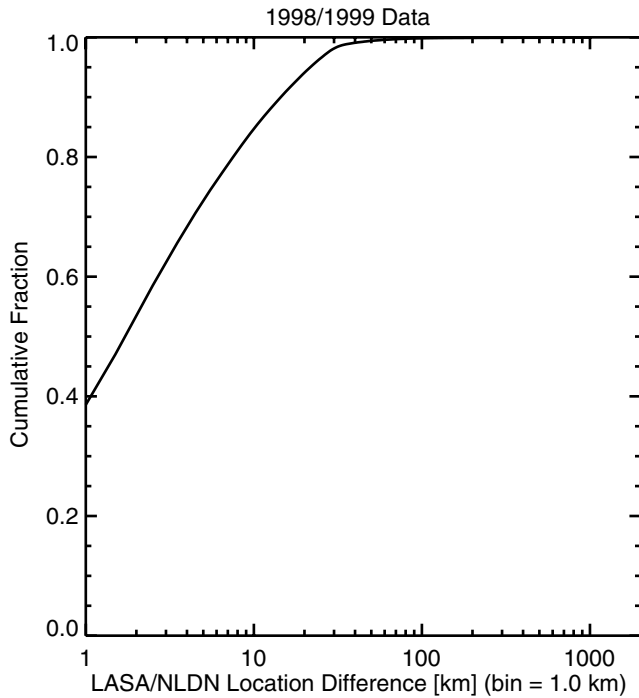
1998/1999 Data

Figure 10. Cumulative log distribution of LASA/NLDN event location differences (1998/1999 data).

intracloud stroke in the loosened criteria database). The LASA convention is to time tag the peak recorded electric field amplitude, which physically corresponds to the time of peak current [*Uman et al.*, 1975]. Peak current typically occurs a few microseconds after return stroke attachment. The second factor is that LASA more often (than NLDN) tags the ionospheric reflections of strokes. The reflection times of arrival are retarded from the groundwave sferics by tens to hundreds of microseconds. On the basis of Figure 9 the time coincidence window for the location analysis was selected to be ±100 µs. The number of events within this window was 497,288.

[38] Figure 10 shows a cumulative log distribution of spatial separations between the LASA and NLDN event locations for events within the ±100 µs coincidence window in the 1998/1999 database. The bin size is 1.0 km. Figure 10 shows that for the entire database, 38% of the LASA/NLDN temporal coincidences agreed to within 1 km, 85% to within 10 km, 99% to within 40 km, and 99.9% to within 220 km.

[39] To determine the extent to which poor LASA locations resulted from geometric dilution of precision, further analysis was performed only on the 1998 array data, since the 1998 NM array was small with a simple geometry (see Figure 1). This allowed us to easily evaluate the effect of event range on location accuracy.

[40] Figure 11 illustrates LASA/NLDN location differences sorted as a function of range from the centroid of the 1998 NM array displayed on a log-log plot. Each 10-km-range bin value indicates the average location difference for all events occurring within the bin limits. Figure 11 shows that on average the event locations agreed to within 1.3 km out to a distance of 70 km from the center of the NM array. The locations agreed to within 2.0 km out to a distance of 130 km, a range that corresponds well to the edge of the

NM array. Beyond the perimeter of the array the array location accuracy decayed steadily to 25 km at a range of 1000 km.

[41] The conclusion with regard to LASA event location accuracy is that events occurring within the NM and FL subarrays were well located, with a mean location error of <2 km. The Florida result was not proven, but we make the argument based on the similar (or even shorter) FL baseline lengths and the better propagation conditions in Florida. Also, both arrays benefited from having five stations in 1999. Within an array diameter outside of the perimeter of each subarray, it is reasonable to expect location accuracy on the order of or better than 10 km. Beyond this distance, the accuracies degrade steadily with distance when the members of the subarray are the only participants in the location determination. Not addressed in this analysis are events detected by members of more than one subarray and/or by the satellite station in Nebraska. Having very distant stations participate in the geolocation solution can be useful in reducing errors, especially when the events to be located lie close to the line between the detecting stations. This is because the distant station constrains the radial component of the location uncertainty, and it is the radial component that grows fastest with distance from the event location.

3.2. Comments on Geolocation Accuracy

[42] The LASA GPS receivers were evaluated prior to deployment and found to produce absolute time tags with a maximum error of <2 µs. On the basis of this measured uncertainty the theoretical achievable location accuracy is better than a kilometer (assuming that the ratio of the location accuracy to the timing accuracy is the speed of light). A number of considerations explain why this accu-
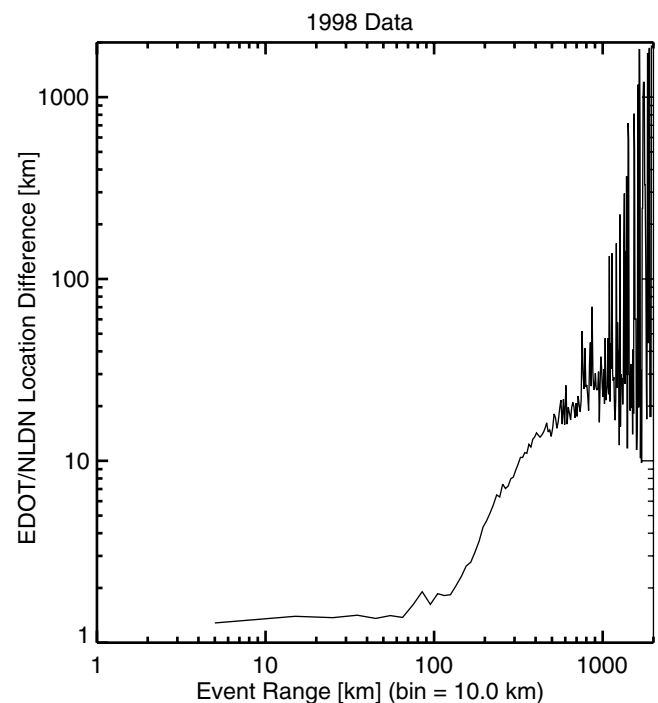
1998 Data

Figure 11. Log-log plot of LASA/NLDN location differences as a function of LASA event range (1998 data).
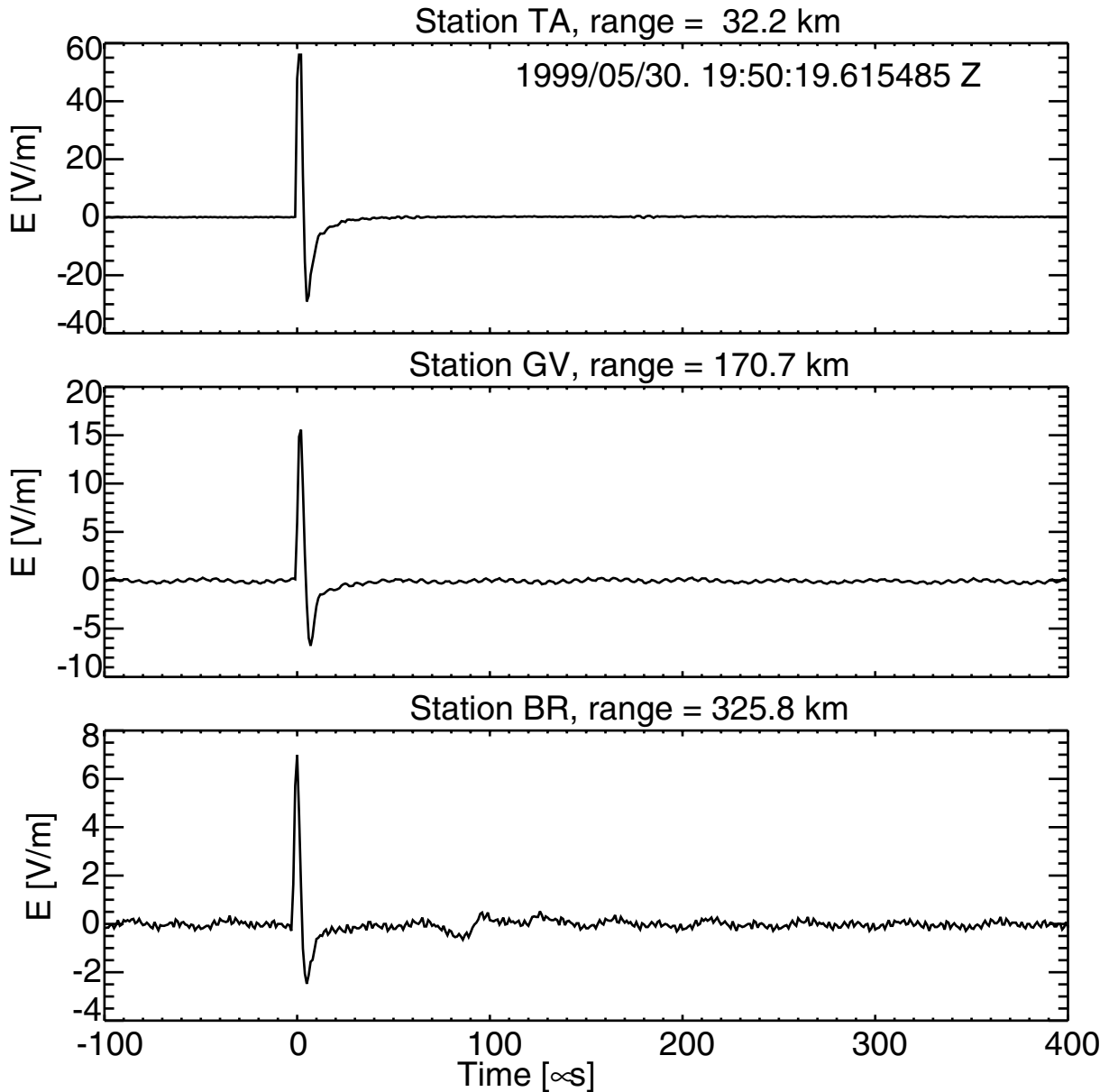
Figure 12. Narrow positive bipolar field change waveforms from a discharge that occurred 32 km northwest of Tampa (the location is indicated by a numeral "3" in Figure 1).

racy was apparently not achieved. The first is that LASA waveform cross correlations are not perfect. With identical waveforms at all stations it would be possible to determine the actual DTOAs to within 1 μs; however, propagation over the finitely conducting ground, ionospheric reflections, and static (near) and inductive (intermediate) field influences all affect the waveshapes. We hypothesized in the discussion of the Figure 6 waveforms that the 2.7-km difference between the LASA and NLDN locations resulted in part from the static contribution evident in the first waveform. Recent modeling and analysis by *Willett et al.* [2000] show that even when the previously mentioned factors are disregarded, channel tortuosity can cause radiation anisotropy as a result of nonvertical channel segments. This anisotropy also degrades waveform cross correlations. A second consideration is that NLDN lightning locations do

not necessarily represent true source locations. The median accuracy for the standard NLDN data product is 0.5 km. The location uncertainty for the loosened criteria data (explained earlier) is not known. A third consideration is the potential for contamination from incidental coincidences. The events used for this comparative study were selected by finding ±100 μs LASA/NLDN coincidences. The 1998 and 1999 NLDN data sets often feature over one million events per day during the summer months. One million events per day corresponds to one every 80 ms. A random event occurring every 80 ms has a 1 in 400 chance of occurring in our ±100-μs window. Incidental NLDN events that occurred simultaneously (or nearly so) with LASA events but that occurred at great distances are included in Figure 11. As a result of geometry, these events are relatively less likely to contaminate the close event
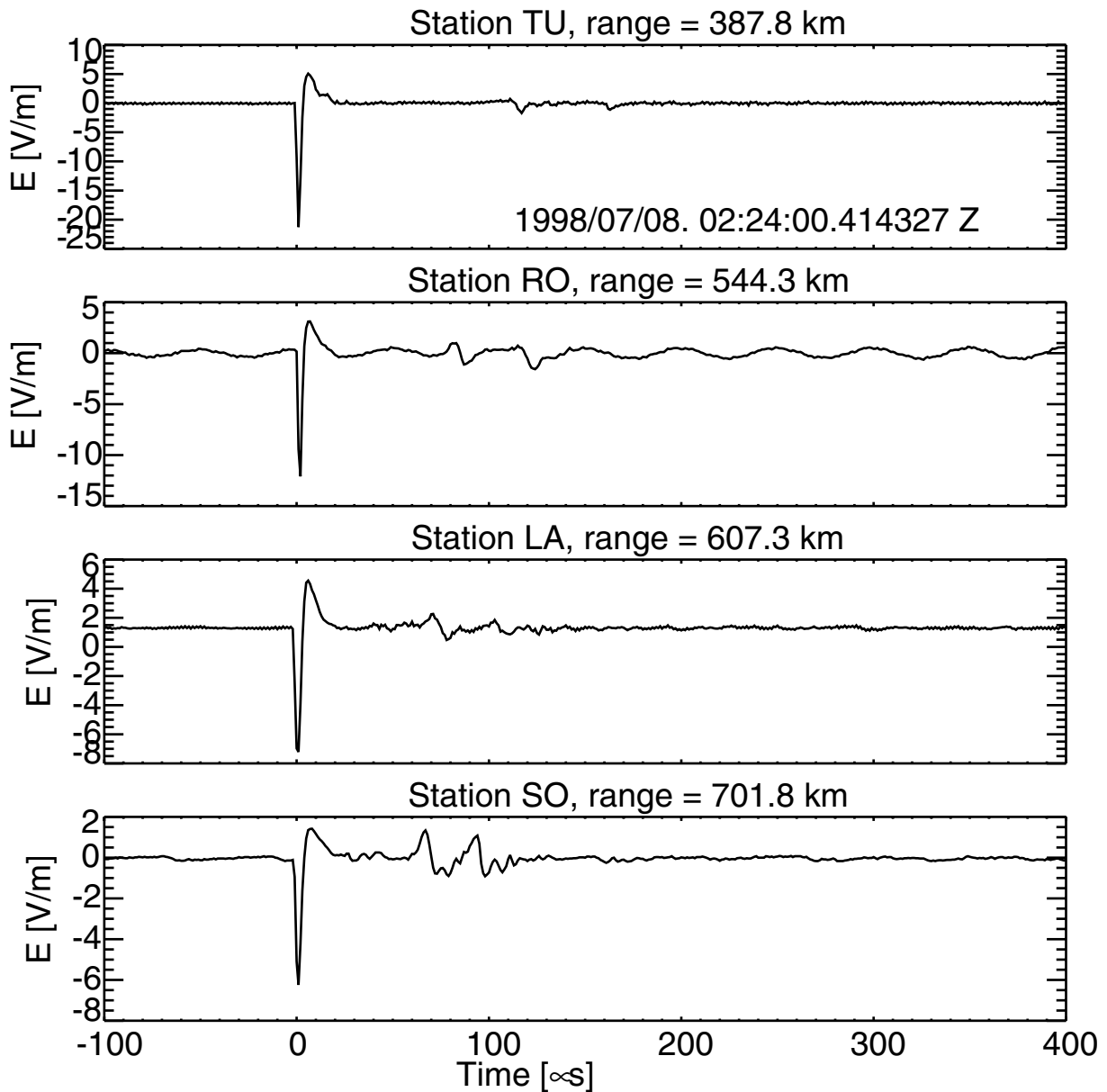
Figure 13. Narrow negative bipolar field change waveforms from a discharge that occurred east of the Texas Panhandle (the location is indicated by a numeral "4" in Figure 1).

range bins than the more distant ones, but the events certainly play a role in the Figure 11 plot beyond several hundred km in range.

4. Identification of Narrow Bipolar Pulses

[43] Narrow bipolar pulses (NBPs) associated with very powerful RF radiation have previously been described by a number of researchers, including *Le Vine* [1980], *Willett et al.* [1989], *Medelius et al.* [1991], *Smith* [1998], *Smith et al.* [1999a], and *Rison et al.* [1999b]. *Smith et al.* [1999a] found that many of the discharges were intracloud events; that is, they occurred at heights above a few km as determined from reflections of field change signals from the Earth and ionosphere. The sources of these fast and isolated bipolar electric field change signatures were referred to as compact intracloud discharges (CIDs). As an extension of the pre-

vious work we attempted to identify waveform qualities that would allow NBPs to be automatically identified in the LASA database. CIDs are excellent targets for FORTE, which regularly records RF radiation from CIDs in the form of transionospheric pulse pairs (TIPPs) [*Holden et al.*, 1995; *Massey and Holden*, 1995; *Massey et al.*, 1998b].

[44] Figures 12 and 13 show LASA examples of NBPs recorded by multiple stations. Figure 12 is a narrow positive bipolar pulse (NPBP) recorded by the Florida TA, GV, and BR stations on May 30, 1999, from distances of 32, 171, and 326 km, respectively. The event occurred northwest of Tampa (the event location is indicated by a "3" in Figure 1). The pulse is shown on a 500-μs timescale, expanded by a factor of 16 compared to the previous waveforms. The pulse is fast and isolated with little evidence of other electrical activity within the waveform (the same is true for the entire 8-ms record). Ionospheric reflections are barely visible in

the BR (Figure 12, bottom) waveform in the neighborhood of 100 μs following the groundwave bipolar pulse. Figure 13 is a narrow negative bipolar pulse (NNBP) recorded by the New Mexico TU, RO, LA, and SO stations on July 8, 1998, from distances of 388, 544, 607, and 702 km, respectively. The event occurred in Oklahoma east of the Texas Panhandle (the event location is indicated by a "4" in Figure 1). Again the pulse is narrow, with a full width at half maximum on the order of 3 μs. Ionospheric reflections are visible in all four waveforms immediately following the groundwave signal. The two reflections correspond to the one-hop ionospheric reflection and the one-hop ionospheric reflection of the ground reflection. The delays are consistent with a source height of 18.6 km and an ionospheric virtual reflection height of 83.4 km. D. A. Smith et al. (Computation of intracloud lightning discharge heights using differential times of arrival of ionospheric and Earth reflections, manuscript in preparation, 2001) describe the methodology for this determination. The most likely explanation as to why the reflections in Figure 12 were weak or nonexistent and the ones in Figure 13 were obvious is that the Figure 12 waveforms were recorded from closer to the source, where the reflections tend to be weaker.

[45] Among the distinguishing characteristics of NBPs are their fast risetimes and fall times and their isolation within our 8-ms-duration electric field change records. It is not unusual to see indications of subsequent IC activity in NBP field change waveforms, but neither is it common. This topic has previously been addressed by *Smith et al.* [1999a, 1999b] and *Rison et al.* [1999a, 1999b]. Figure 14 is a scatterplot of event rise-plus-fall time versus waveform signal-to-noise ratio (SNR) for the entire 1998 LASA waveform database. The determination of risetime is made by extrapolating to zero the line determined by the peak absolute amplitude of the waveform and the first point prior to the peak that exceeds 10% of that amplitude. The risetime is defined as the time
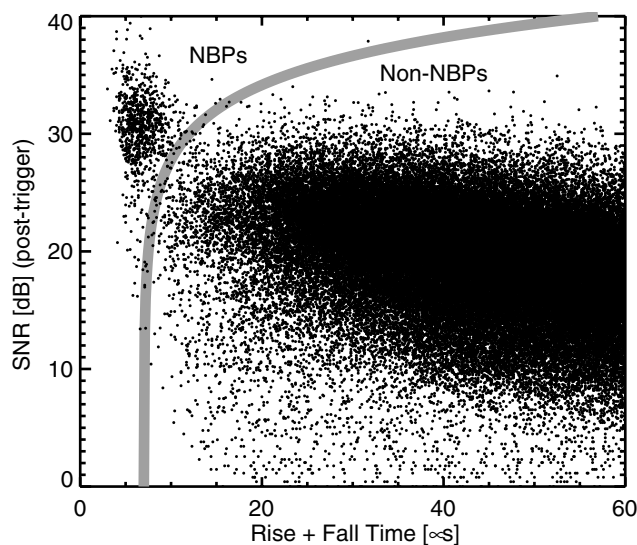
Table 2. Compilation of Statistics on Positive and Negative Narrow Bipolar Pulses (NPBPs and NNBPs) in 1998 and 1999

	1998	1999
Total Events	135,835	765,208
NPBPs	728	8462
NNBPs	134	3568

between the extrapolated zero crossing and the peak absolute amplitude. The fall time is the time between the peak amplitude and the first point to cross zero toward the opposite waveform polarity. The SNR for this study was computed by calculating the ratio of the average power within ±5 μs of the trigger point to the average power in the waveform from 6 μs after the trigger point to the end of the record. Once these parameters have been determined for each waveform that comprises an event, they are determined for the event itself. This was done by taking the average rise-plus-fall time and the minimum SNR. The minimum SNR was used rather than the average because local noise in waveforms at some stations significantly reduced NBP SNRs. The rise-plus-fall times in Figure 14 are in microseconds. The SNRs are in decibels. Two populations are evident in the scatterplot, providing a quantitative basis for identifying CID electric field change waveforms. The minor cluster in the upper left corner of Figure 14 represents NBPs, as verified by our observations of the waveforms. The large cluster of events on the lower right side of Figure 14 includes everything else and represents the vast majority (99.3%) of events recorded during 1998. The shaded line in Figure 14 was used to automatically classify events as NBPs or non-NBPs in the LASA database. Polarities of bipolar pulses were determined by assigning the polarity of the first point following the trigger point to the waveform. Table 2 presents the distribution of NNBPs, NPBPs, and other events recorded in 1998 and 1999 as determined from the classification methods described in this section. *Smith et al.* [1999a] did not report or record any observations of NBPs of initially negative polarity (both polarities had been reported by *Willett et al.* [1989]). Table 2 shows that negatives comprised 29% of the total number of NBPs recorded by the sferic array in 1998 and 1999.

5. Summary

[46] Motivation for the deployment of the Los Alamos Sferic Array was provided by the FORTE satellite project, which has a need for ground truth data that add value by providing the locations of events detected by FORTE, by further characterizing the events, and by providing background data when FORTE is not overhead. The sferic array now provides continuous coverage of lightning by providing event locations and limited event classifications. These data go back to May of 1998 when the array became operational. In the future the array will provide more comprehensive event classifications, as well as characterizations of event physical parameters. These expanded data sets will be applicable to the entire archive of sferic data, since all waveforms have been retained since array inception. This paper has described some of the initial event

Figure 14. Scatterplot of rise-plus-fall time versus signal-to-noise ratio (in decibels) for all 1998 LASA events. The shaded line between the two populations indicates our criterion for classification of NBPs.

location and identification capabilities and has provided a quantitative evaluation of its location accuracy.

References

Boccippio, D. J., S. Heckman, and S. J. Goodman, A diagnostic analysis of the Kennedy Space Center LDAR network, 1, Data characteristics, *J. Geophys. Res.*, *106*(D5), 4769–4786, 2001.

Cummins, K. L., M. J. Murphy, E. A. Bardo, W. L. Hiscox, R. B. Pyle, and A. E. Pifer, A combined TOA/MDF technology upgrade of the U.S. National Lightning Detection Network, *J. Geophys. Res.*, *103*(D8), 9035–9044, 1998a.

Cummins, K. L., E. P. Krider, and M. D. Malone, The U.S. National Lightning Detection Network and applications of cloud-to-ground lightning data by electric power utilities, *IEEE Trans. Electromagn. Compat.*, *40*(4), 1998b.

Holden, D. N., C. P. Munson, and J. C. Devenport, Satellite observations of transionospheric pulse pairs, *Geophys. Res. Lett.*, *22*, 889–892, 1995.

Jacobson, A. R., and X. M. Shao, Using geomagnetic birefringence to locate sources of impulsive, terrestrial VHF signals detected by satellites on orbit, *Radio Sci.*, *36*(4), 671–680, 2000.

Jacobson, A. R., S. O. Knox, R. Franz, and D. C. Enemark, FORTE observations of lightning radio-frequency signatures: Capabilities and basic results, *Radio Sci.*, *34*(2), 337–354, 1999.

Jacobson, A. R., K. L. Cummins, M. Carter, P. Klingner, D. Roussel-Dupré, and S. O. Knox, FORTE radio-frequency observations of lightning strokes detected by the National Lightning Detection Network, *J. Geophys. Res.*, *105*(D12), 15,653–15,662, 2000.

Kirkland, M. W., D. M. Suszcynsky, R. Franz, J. L. L. Guillen, and J. L. Green, Observations of terrestrial lightning at optical wavelengths by the photodiode detector on the FORTE satellite, *Rep. LA-UR-98-4098*, Los Alamos Natl. Lab., Los Alamos, N. M., 1998.

Krehbiel, P. R., M. Brook, and R. A. McCrory, An analysis of the charge structure of lightning discharges to ground, *J. Geophys. Res.*, *84*(C5), 2432–2456, 1979.

Lee, A. C. L., Ground truth confirmation and theoretical limits of an experimental VLF arrival time difference lightning flash locating system, *Q. J. R. Meteorol. Soc.*, *115*, 1147–1166, 1989.

Lennon, C., and L. Maier, Lightning mapping system, in *Proceedings of the International Aerospace and Ground Conference on Lightning and Static Electricity, NASA Conf. Publ.*, *3106*, 89-1–89-10, 1991.

Le Vine, D. M., Sources of the strongest RF radiation from lightning, *J. Geophys. Res.*, *85*, 4091–4095, 1980.

Light, T. E., D. M. Suszcynsky, M. W. Kirkland, and A. R. Jacobson, Simulations of lightning optical waveforms as seen through clouds by satellites, *J. Geophys. Res*, *106*(D14), 17,103–17,114, 2001.

Massey, R. S., and D. N. Holden, Phenomenology of transionospheric pulse pairs, *Radio Sci.*, *30*(5), 1645–1659, 1995.

Massey, R. S., S. O. Knox, R. C. Franz, D. N. Holden, and C. T. Rhodes, Measurements of transionospheric radio propagation parameters using the FORTE satellite, *Radio Sci.*, *33*(6), 1739–1753, 1998a.

Massey, R. S., D. N. Holden, and X. M. Shao, Phenomenology of transionospheric pulse pairs: Further observations, *Radio Sci.*, *33*(6), 1755–1761, 1998b.

Medelius, P. J., E. M. Thomson, and J. S. Pierce, E and DE/DT waveshapes for narrow bipolar pulses in intracloud lightning, in *Proceedings of the International Aerospace and Ground Conference on Lightning and Static Electricity, NASA Conf. Publ.*, *3106*, 12-1–12-10, 1991.

Nelder, J. A., and R. Mead, A simplex method for function minimization, *Comp. J.*, *7*, 308–313, 1965.

Pinto, O., Jr., I. R. C. A. Pinto, J. H. Diniz, A. M. Caravalho, and A. C. Filho, Cloud-to-ground lightning flash characteristics obtained in southeastern Brazil using the LPATS technique and the new hybrid lightning location methodology, in *Proceedings of the 11th International Conference on Atmospheric Electricity*, edited by H. Christian, *NASA Conf. Publ.*, *209261*, 62–64, 1999.

Press, W. H., B. P. Flannery, S. A. Teukolsky, and W. T. Vetterling, Downhill simplex method in multidimensions, in *Numerical Recipes*, pp. 289–293, Cambridge Univ. Press, New York, 1986.

Proctor, D. E., A hyperbolic system for obtaining VHF radio pictures of lightning, *J. Geophys. Res.*, *76*(6), 1478–1489, 1971.

Rison, W., R. Scott, R. J. Thomas, P. R. Krehbiel, T. Hamlin, and J. Harlin, 3-dimensional lightning and dual-polarization radar observations of thunderstorms in central New Mexico, in *Proceedings of the 11th International Conference on Atmospheric Electricity*, edited by H. Christian, *NASA Conf. Publ.*, *209261*, 432–435, 1999a.

Rison, W., R. J. Thomas, P. R. Krehbiel, T. Hamlin, and J. Harlin, A GPS-based three-dimensional lightning mapping system: Initial observations in central New Mexico, *Geophys. Res. Lett.*, *26*, 3573–3576, 1999b.

Shao, X. M., and A. R. Jacobson, Polarization observations of broadband VHF signals by the FORTE satellite, *Radio Sci.*, *36*(6), 1573–1590, 2001.

Smith, D. A., Compact intracloud discharges, Ph.D. dissertation, Dep. of Electr. Eng., Univ. of Colo., Boulder, 1998.

Smith, D. A., X. M. Shao, D. N. Holden, C. T. Rhodes, M. Brook, P. R. Krehbiel, M. Stanley, W. Rison, and R. J. Thomas, A distinct class of isolated intracloud lightning discharges and their associated radio emissions, *J. Geophys. Res.*, *104*(D4), 4189–4212, 1999a.

Smith, D. A., R. S. Massey, K. C. Wiens, K. B. Eack, X. M. Shao, D. N. Holden, and P. E. Argo, Observations and inferred physical characteristics of compact intracloud discharges, in *Proceedings of the 11th International Conference on Atmospheric Electricity*, edited by H. Christian, *NASA Conf. Publ.*, *209261*, 6–9, 1999b.

Suszcynsky, D. M., M. Kirkland, P. Argo, R. Franz, A. Jacobson, S. Knox, J. Guillen, J. Green, and R. Spalding, Thunderstorm and lightning studies using the FORTE optical lightning system (FORTE/OLS), in *Proceedings of the 11th International Conference on Atmospheric Electricity*, edited by H. Christian, *NASA Conf. Publ.*, *209261*, 672–675, 1999.

Suszcynsky, D. M., M. W. Kirkland, A. R. Jacobson, R. C. Franz, S. O. Knox, J. L. L. Guillen, and J. L. Green, FORTE observations of simultaneous VHF and optical emissions from lightning: Basic phenomenology, *J. Geophys. Res.*, *105*(D2), 2191–2201, 2000.

Suszcynsky, D. M., T. E. Light, S. Davis, J. L. Green, J. L. L. Guillen, and W. Myre, Coordinated observations of optical lightning from space using the FORTE photodiode detector and CCD imager, *J. Geophys. Res.*, *106*(D16), 17,897–17,906, 2001.

Uman, M. A., D. K. McLain, and E. P. Krider, The electromagnetic radiation from a finite antenna, *Am. J. Phys.*, *43*, 33–38, 1975.

Willett, J. C., J. C. Bailey, and E. P. Krider, A class of unusual lightning electric field waveforms with very strong high-frequency radiation, *J. Geophys. Res.*, *94*(D13), 16,255–16,267, 1989.

Willett, J. C., D. A. Smith, and D. M. Le Vine, Geometrical effects on the electromagnetic radiation from lightning return strokes (abstract), *EOS Trans. AGU*, *81*(48), Fall Meet. Suppl., F89, 2000.

————————

K. B. Eack and J. Harlin, Langmuir Laboratory for Atmospheric Research, New Mexico Institute of Mining and Technology, 801 Leroy Place, Socorro, NM 87801, USA. (keack@kestrel.nmt.edu; jharlin@nmt.edu)

M. J. Heavner, A. R. Jacobson, X. M. Shao, and D. A. Smith, Space and Atmospheric Sciences, Los Alamos National Laboratory, NIS-1, MS D466, Los Alamos, NM 87545, USA. (heavner@lanl.gov; ajacobson@lanl.gov; xshao@lanl.gov; dasmith@lanl.gov)

K. C. Wiens, Department of Atmospheric Science, Colorado State University, Fort Collins, CO 80521-1371, USA. (kwiens@atmos.colostate.edu)
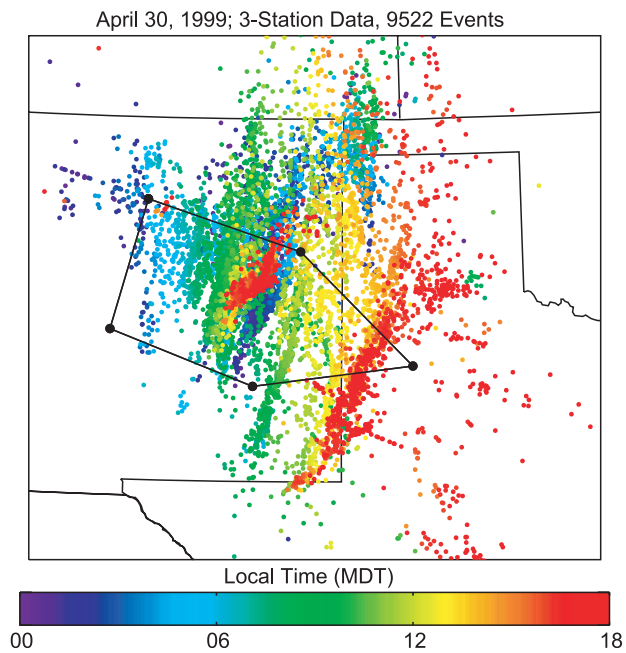
April 30, 1999; 3-Station Data, 9522 Events

Local Time (MDT)

00   06   12   18

Figure 7. Map of array activity recorded in the vicinity of the NM subarray on April 30, 1999. Color is indicative of local time of day (MDT).

December 12-13, 1999; 4-Station Data, 14366 Events

Local Time (CST)

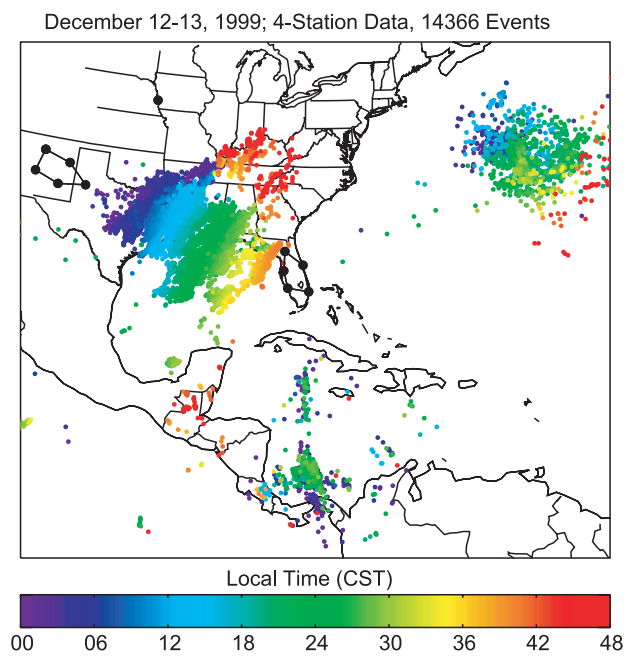00   06   12   18   24   30   36   42   48

Figure 8. Map of all array activity recorded on December 12–13, 1999. Color is indicative of local time of day (central standard time). The map demonstrates the long-range detection capability of the sferic array when the thresholds are low.